

Numerical simulation of detonation wave propagation in a non-uniform medium in the shock-attached frame

Alexander I. Lopato
Institute for Computer Aided Design of RAS
Moscow, Russian Federation

Yaroslava E. Poroshyna
Queen's University
Kingston, Canada

Pavel S. Utkin
Harbin Institute of Technology
Harbin, China

1 Introduction

Propagation of detonation waves (DW) in non-uniform gaseous mixtures has become a matter of interest over the past several years due to the development of rotating detonation engines. In practice, an oxidizer and a fuel are injected into the combustion chamber separately. It leads to the propagation of a detonation through a highly inhomogeneous mixture.

In order to understand a real-life process of detonation propagation in a non-uniform environment, some simplified settings have been studied: (i) DW propagation in a mixture with a longitudinal or transverse gradient of fuel concentration, (ii) DW propagation in a mixture with varying density, heat release or other parameters, (iii) DW propagation along or across an inert gas layer, (iv) analog modeling of detonation dynamics, see [1 – 3] as a few latest examples most relevant to the current work.

In our previous works, we constructed the numerical algorithms for one-dimensional (1D) pulsating DW simulations in the shock-attached frame (SAF) using a one-stage [4] and a two-stage [5] chemical kinetics model. The algorithms further develop the approach from [6]. SAF simulations are well suited for the stability studies and characteristics analysis of pulsating DW. The computational burden in SAF simulations is significantly less than that for common approaches as the computational domain is always only a small area behind the DW front. In addition, they provide exact (i.e. without numerical smearing) parameters behind the leading shock wave (LSW).

Here, we decided to further develop the numerical algorithm for the DW simulation in SAF for the case of a non-uniform distribution of parameters in front of the DW. Namely, the varying gas density was considered as in [2]. The algorithm was used for the characteristics analysis of the stable DW propagation in a non-uniform medium.

2 Mathematical Model

The mathematical model was based on the 1D Euler equations written in the shock-attached frame (x, t) supplemented by a one-stage chemical kinetics model:

$$\begin{aligned} \frac{\partial \mathbf{u}}{\partial t} + \frac{\partial}{\partial x}(\mathbf{f} - D\mathbf{u}) &= \mathbf{s}, \quad x = x' - \int_0^t D dt, \\ \mathbf{u} &= \begin{bmatrix} \rho \\ \rho v \\ e \\ \rho Z \end{bmatrix}, \quad \mathbf{f} = \begin{bmatrix} \rho v \\ \rho v^2 + p \\ (p + e)v \\ \rho v Z \end{bmatrix}, \quad \mathbf{s} = \begin{bmatrix} 0 \\ 0 \\ -\rho Q \omega \\ \rho \omega \end{bmatrix}, \\ e &= \rho \varepsilon + \frac{1}{2} \rho v^2, \quad \varepsilon = \frac{p}{\rho(\gamma - 1)}, \quad \omega = -AZ \exp\left(\frac{-E\rho}{p}\right). \end{aligned} \quad (1)$$

Here, ρ is the density, v is the velocity in the laboratory frame (x', t) , D is the LSW velocity, p is the pressure, Q is the heat release of the chemical reactions, Z is the mass fraction of the reactive component of the mixture, ω is the rate of chemical reactions, e is the total energy per the unit of volume, ε is the specific internal energy of the gas, A is the pre-exponential factor, E is the activation energy. The gas was considered to be ideal with the specific heat ratio γ . The defining equations were rescaled following the traditional convention [7] using a half-reaction length and parameters in front of the DW as characteristic scales.

The LSW speed was obtained by integrating the governing equations along the C_+ characteristic near the shock [6] taking into account the varying gas density in front of the shock:

$$\begin{cases} \frac{dp}{dt} + \rho c \frac{dv}{dt} - (\gamma - 1)Q\rho\omega = 0, \\ \frac{dx}{dt} = v + c - D, \\ \rho_0 = \rho_0 \left(x'_0 + \int_0^t D(\tau) d\tau \right). \end{cases} \quad (2)$$

Here, d/dt in the first equation is the material derivative along the C_+ characteristic. The density ahead of the shock ρ_0 was considered to be a known function of the spatial coordinate in a laboratory frame. Parameter x'_0 denotes the initial coordinate of the LSW.

3 Computational algorithm

The computational domain was a segment which was covered by a uniform grid with N cells. The length of the segment was chosen to eliminate the influence of the rear boundary on the LSW dynamics [5] even for the zero-order extrapolation boundary condition. Rankine-Hugoniot jump conditions were set on the right boundary of the domain. The Zel'dovich-von Neumann-Döring solution was used as the initial conditions. The finite-volume numerical algorithm was described in detail in [4]. The main improvement in the numerical approach was the method of integrating the system (2) due to the non-uniform distribution of density. The system was discretized the following way:

$$\begin{cases} p_s^{n+1} - p_s^n + 0.5 \left((\rho c)_s^n + (\rho c)_s^{n+1} \right) (v_s^{n+1} - v_s^n) - (\gamma - 1)Q\rho_s^{n+1}\omega_s^{n+1}\Delta t^n = 0, \\ -x_s^n = (c_s^n + v_s^n - D^n)\Delta t^n \\ \rho_0^{n+1} = \rho_0(x_0 + L^n + c_0^{n+1}M^{n+1}\Delta t^n). \end{cases} \quad (3)$$

The subscript s denotes parameters behind the LSW at $x_s = 0$; L^n is the distance traveled by the LSW at t^n . The star subscript denotes the point of intersection of C_+ characteristics with x axis. Parameters at this point were computed using the linear interpolation between the known parameters at $x_N = -\Delta x/2$ and at $x_s = 0$, see [4] for the details. The coordinate x_*^n was found from the second equation of the system (3):

$$x_*^n = -\frac{c_s^n + v_s^n - D^n}{1 + \frac{2\Delta t^n}{\Delta x}(c_s^n - c_N^n + v_s^n - v_N^n)} \cdot \Delta t^n.$$

The remaining equations

$$\begin{cases} p_s^{n+1} - p_*^n + \frac{1}{2}((\rho c)_*^{n+1} + (\rho c)_s^{n+1})(v_s^{n+1} - v_*^n) - (\gamma - 1)Q\rho_s^{n+1}\omega_s^{n+1}\Delta t^n = 0, \\ \rho_0^{n+1} - \rho_0(x_0 + L^n + \sqrt{\gamma p_0^{n+1}/\rho_0^{n+1}}M^{n+1}\Delta t^n) = 0, \end{cases}$$

were solved using the Newton method with unknown variables ρ_0^{n+1} and M^{n+1} since p_s^{n+1} , ρ_s^{n+1} , v_s^{n+1} and ω_s^{n+1} depended on these two variables.

4 Verification of the algorithm. Shu-Osher problem.

The computational algorithm for the inert case was verified in [8] for two types of inhomogeneities in front of the LSW: a segment of finite length with a linear density gradient and a sinusoidal density distribution. For the case of a linear gradient, the obtained results were compared with the analytical Chisnell–Whitham theory, which did not take into account the effect of re-reflected waves on the LSW. Good agreement was obtained for the case of decreasing density in front of the SW and discrepancy was obtained between the results for the case of increasing density, which was due to the different degrees of influence of re-reflected waves on the LSW.

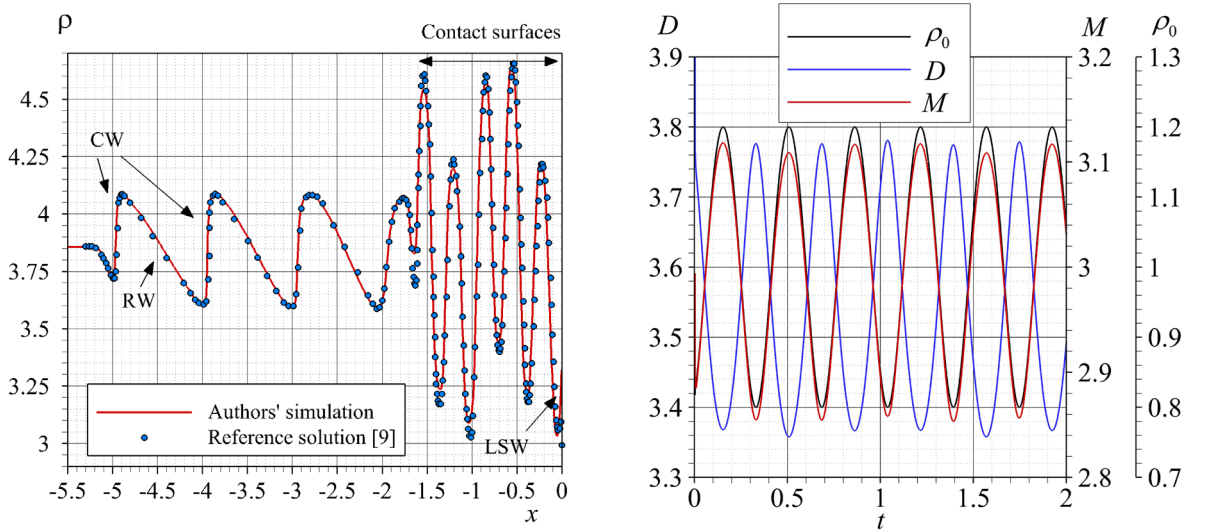


Figure 1: Shu-Osher problem simulation. Left: Density profile at the time instant $t = 1.8$. Right: Evolution of shock velocity, shock Mach number and density in front of the LSW in time.

Consider the problem of an inert moving shock wave interaction with sine waves in density (we call it Shu-Osher problem [9]). This test is important for the verification of the SAF numerical algorithm. It

is also important to establish the “gasdynamics” mechanism of the LSW – density perturbations interaction for the subsequent analysis of additional “reactive” mechanisms for the case of DW simulation. The characteristics analysis like in [5, 10] was is used.

At the initial time moment, the whole computational domain is filled with the air with the parameters behind the shock wave with Mach number $M = 3.0$ for $p_0 = 1.0$, $v_0 = 0.0$, $\rho_0 = 1.0$. The length of the domain L is equal to 20 and $N = 4000$. The density in the domain changes according to the following law:

$$\rho_0 = 1.0 + 0.2 \cdot \sin\left(-20.0 + 5.0 \cdot \int_0^t D(\tau) d\tau\right).$$

The interaction of the LSW with sine waves leads to the oscillating solution (Figure 1). Eventually, each wave front becomes steeper and a shock train is formed behind the LSW front. However, for earlier moments, the solution behind the shock remains smooth. It can be seen from Figure 1 Left that the density profiles calculated by the authors and profiles from [9] coincide except for several peak amplitudes in the region of contact surfaces.

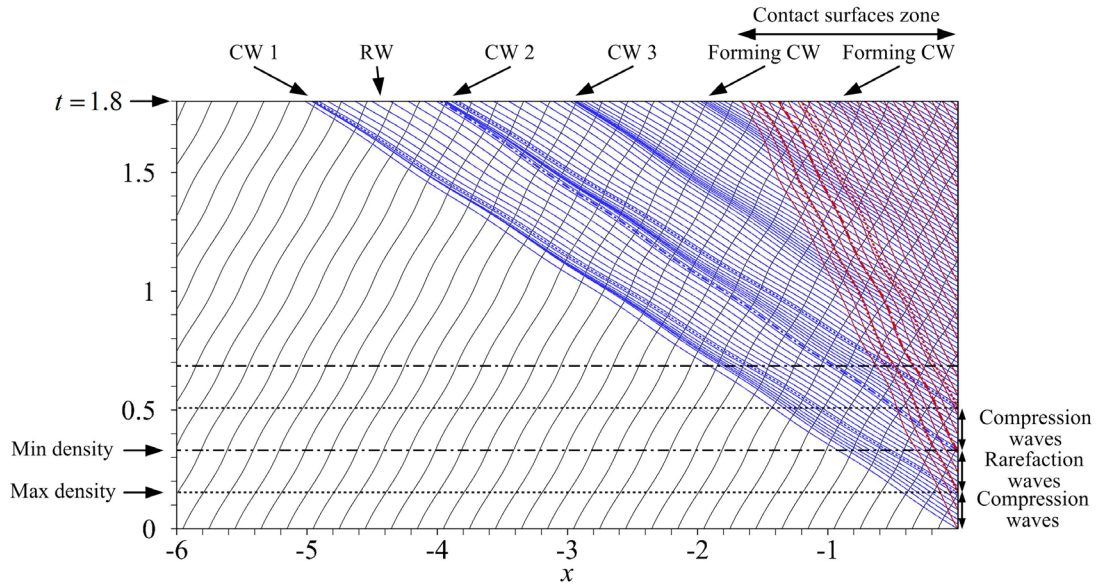


Figure 2: Characteristics in the Shu-Osher problem [9]. Black lines denote C_+ characteristics, blue lines are C_- characteristics, red lines are C_0 characteristics.

At the initial moment of time and up to the moment $t \approx 0.154$, the density in front of the LSW increases according to the sinusoidal law. As in the problem with a linearly growing density ahead of the LSW front [8], this is accompanied by the formation of compression waves (CW) and contact discontinuities (Figure 2). In this case, the Mach number of the LSW increases, while its speed decreases. Waves reflected from the LSW and following along the characteristics C_- , gradually merge into one characteristic, catching up with each other. The compression wave front becomes steeper with time. As a result, this process leads to the formation of internal SWs, shocklets. At the point in time $t \approx 0.154$ the density in front of the LSW begins to decrease, and, similarly to the case of a decreasing linear density gradient [8], now rarefaction waves (RW) follow along the characteristics C_- ; and the LSW starts accelerating, and its Mach number decreases. Further, the process is repeated cyclically.

5 Detonation wave propagation in a medium with varying density

Now let’s consider interaction of a stable DW ($Q = 50.0$, $E = 25.0$, $\gamma = 1.2$) with sine waves in density. Parameters in front of the LSW are the following:

$$p_0 = 1.0, v_0 = 0.0, \rho_0 = 1.0 + 0.1 \cdot \sin\left(\frac{2\pi}{\lambda} \cdot \int_{t_1}^t D(\tau) d\tau\right).$$

The Chapman-Jouguet detonation velocity D_{CJ} for the chosen values of Q and γ is approximately 6.81. Linear theory predicts that the DW is stable for $E < 25.26$. The length of the channel L is equal to 20 and the number of cells N is 2000. The CFL number is equal to 0.1.

The numerical algorithm for the DW simulation in SAF was also verified using the data from [2] for two regimes with $\lambda = 100$ and $\lambda = 190$ ($E = 28.5$). Pressure pulsation characteristics were in good agreement.

Consider in more detail simulation results for $\lambda = 25.0$. Initially, a stable propagation mode of DW for the uniform background density $\rho_0 = 1.0$ was obtained. After that, at the time moment $t_1 = 500.0$, the density starts changing sinusoidally.

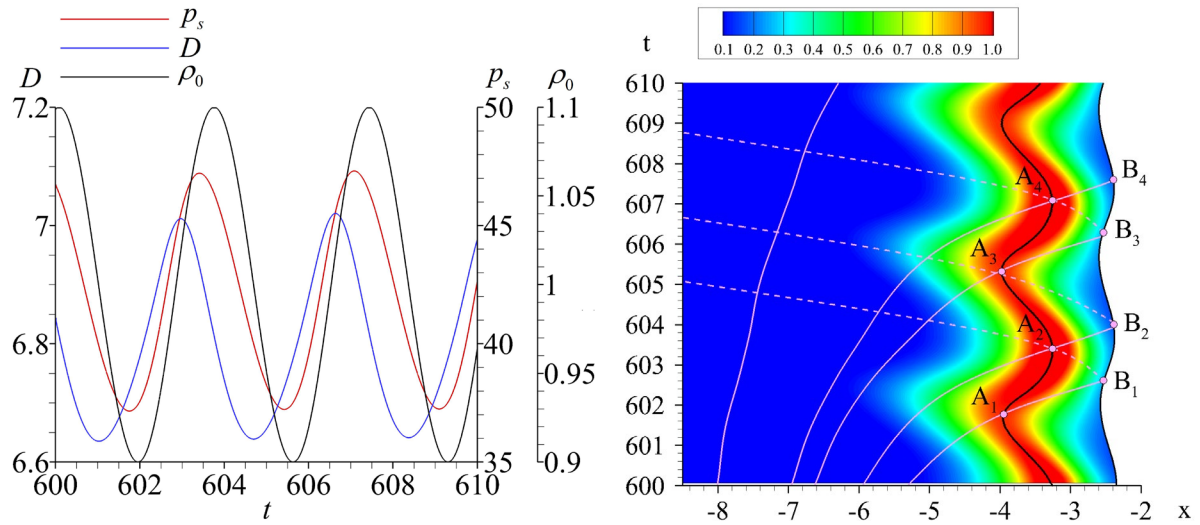


Figure 3: The dynamics of a stable DW propagation. Left: evolution of shock pressure p_s , shock velocity D and density in front of the shock ρ_0 . Right: the rate of chemical reaction contour plotted on the x - t diagram in a reference frame moving with D_{CJ} with C_+ (pink solid lines) and C_0 (pink dotted lines) characteristics. The line $A_1A_2A_3A_4$ denotes the maxima of the rate of chemical reactions.

The obtained regime corresponded to the “surfing” mode from [3]. It means that the DW follows the ambient state oscillations. Oscillations of the parameters such as LSW pressure and LSW velocity occurred with the same period as the gas density in front of the LSW, although they are out of sync with each other, see Figure 3 Left. In the present study, since a one-stage kinetics model is used, the reaction zone is infinite and affects the LSW all the time with the maxima of $|\omega|$ regularly approaching closely and moving away from the LSW. Therefore, the process of formation of pulsations can be explained by combination of the “reactive” and “gasdynamics” (similar to the Shu-Osher problem, described above) mechanisms occurring simultaneously.

Characteristics analysis explains the asynchronous behavior of the curves in Figure 3 Left. Points $A_1 - A_4$ are denoted on the line of the maximal rate of chemical reactions in Figure 3 Right. The area to the right from this line can be considered as the effective induction zone. Points A_1 and A_3 are the most long-distance ones from the LSW while A_2 and A_4 are the closest to the LSW. C_+ characteristics emitted from points $A_1 - A_4$ come to the LSW at point $B_1 - B_4$. As a result of the conducted characteristics analysis, it was shown that one cycle of parameter fluctuations behind the DW front can be schematically decomposed into two passes of characteristics C_+ and two passes of characteristics C_0 along the effective induction zone. We can also see that the phase shift between the curves of the oscillation of the velocity of the DW and the density of the gas before the wave (Figure 3 Left) can be

estimated as the maximum time of passage of the characteristic C_+ through the induction zone, $\Delta t_{\max} \approx t_{B_1} - t_{A_1} \approx 0.8$ (see Figure 3 Right).

6 Conclusion

We developed the algorithm for the simulation of detonation wave propagation in a medium with varying density in the shock-attached frame using a one-stage model of kinetics of chemical reactions. The algorithm was verified on the Shu-Osher problem solution (simulation of interaction of a shock wave with sine waves in density). Using the algorithm and characteristics analysis, we described a stable mode of detonation propagation ($E = 25.0$) in the sinusoidal density field. Characteristics analysis explains time dependencies of the leading shock wave pressure and velocity in terms of acoustic wave propagation inside an effective induction zone behind the leading shock wave. Apparently, the analysis using a model with finite reaction zone length where the heat release is more localized than in the current model (for example, two-step chain-branching model) would be more appropriate to establish quantitative mechanisms of the process.

The work of A. Lopato was supported by the Russian Science Foundation (project No. 22-71-00113). Yaroslava E. Poroshyna carried out her part of the work when she was a student at the Moscow Institute of Physics and Technology.

References

- [1] Ma WJ, Wang C, Han WH. (2020). Effect of concentration inhomogeneity on the pulsating instability of hydrogen–oxygen detonations. *Shock Waves*. 30: 703.
- [2] Kim M, Mi XC, Kiyanda CB, Ng HD. (2021). Nonlinear dynamics and chaos regularization of one-dimensional pulsating detonations with small sinusoidal density perturbations. *Proc. Combust. Inst.* 38: 3701
- [3] Kasimov AR, Goldin AYu. (2021). Resonance and mode locking in gaseous detonation propagation in a periodically nonuniform medium. *Shock Waves*. 31: 841.
- [4] Lopato AI, Utkin PS. (2016). Toward second-order algorithm for the pulsating detonation wave modeling in the shock-attached frame. *Comb. Sci. Tech.* 188: 1844
- [5] Poroshyna YE., Lopato AI, Utkin PS. (2021). Nonlinear dynamics of pulsating detonation wave with two-stage chemical kinetics in the shock-attached frame. *J Inv. Ill-posed Probl.* 29: 557.
- [6] Kasimov AR, Stewart DS. (2004). On the dynamics of self-sustained one-dimensional detonations: A numerical study in the shock-attached frame. *Phys. Fluids*. 16: 3566.
- [7] Erpenbeck JJ. (1962). Stability of steady-state equilibrium detonations. *Phys. Fluids*. 5: 604.
- [8] Poroshyna YaE, Lopato AI, Utkin PS. (2022). Characteristic analysis of the dynamics of shock wave propagation in a medium with a nonuniform density distribution. *Russ. J. Phys. Chem. B*. 16: 670.
- [9] Shu CW, Osher S. (1989). Efficient implementation of essentially nonoscillatory schemes, II. *J. Comput. Phys.* 83: 32.
- [10] Leung C, Radulescu MI, Sharpe GJ. (2010). Characteristics analysis of the one-dimensional pulsating dynamics of chain-branching detonations. *Phys. Fluids*. 22: 126101.